ETEAPOT EDM Benchmark I: Updated Results:

J. D. Talman and R. M. Talman

November 6, 2019

Abstract

This chapter repeats and updates benchmark lattice investigations first performed using the "all-electric" code ETEAPOT in 2012 for all-electric proton EDM rings. The lattice electric bending fields for the three files have indices $m = -1$, $m \approx 0$, and $m = 1$. Values of horizontal and vertical tunes, and beta functions at the origin (midway between adjacent bends) are tabulated. Results are compared to values obtained from a linearized transfer matrix formalism. In all cases the design vertical tunes have been adjusted to Q_y=0.2.

1 Introduction

All-electric lattices for a storage ring to measure the electric dipole moment (EDM) of the proton are described in a CERN Yellow Report, CERN-2019-001-M, "Feasibility Study for a Storage Ring to Search for EDMs of Charged Particles". Earlier designs were contained in a BNL proposal by the Storage Ring EDM Collaboration, *A Proposal to Measure the Proton Electric Dipole Moment with 10^{-29} e-cm Sensitivity*[1]. The lattices studied here have been stripped down to their bare essentials in order to simplify benchmark comparisons of various simulation codes. All results using ETEAPOT in an (unpublished) 2012 benchmark report (to the DOE, in connection with their financial support at the time) are replicated using (updated) ETEAPOT in the present report.

An electric field with index m power law dependence on radius r, for $y=0$, is

$$\mathbf{E}(r,0) = -E_0 \frac{r_0^{1+m}}{r^{1+m}} \, \hat{\mathbf{r}}, \tag{1}$$

and the electric potential $V(r)$, adjusted to vanish (on the storage ring design orbit) at $r = r_0$, is

$$V(r) = -\frac{E_0 r_0}{m} \left(\frac{r_0^m}{r^m} - 1 \right). \tag{2}$$

The "cleanest" case theoretically has $m=1$, in which case it is known as the Kepler or the Coulomb electric field. Our problem is a bit more general than this non-reletivistic terminology suggests, since our treatment is necessarily relativistic. For $m=1$ the Kepler problem can be solved with the same generality in the relativistic as in the nonrelativistic case; but the orbits are no longer exactly elliptical, nor exactly closed however[3].

The full rings simulated in this chapter are circular and consist of 40 identical cells. A single cell is shown in Figure 1. With curved planar plates (which is the easiest configuration to construct) the electrodes are concentric cylinders and the field index is $m=0$. The optimal (i.e. longest) spin coherence time (SCT) is expected to be close to this zero m-value. (For $m=1$ the electrodes would be concentric spheres.)

For $m=0$ the fields are independent of vertical displacement y, which implies that there is no vertical focusing provided by the bending field. Provision of vertical stability therefore requires focusing quadrupoles; they are labeled q in Figure 1. Even if not required for vertical stability, the q quadrupoles are necessary for adjusting the vertical tune Q_y of the storage ring. The vertical tunes have been adjusted to $Q_y = 0.2$ for all three of the benchmark lattices described in the following sections.

2 Parameters of Benchmark Lattices

Analytic, linearized transfer matrix MAPLE programs with names E_BM_P1.0.mw, E_BM_Z.mw, and E_BM_M1.0.mw are in /home/talman/EDM/EDM-lattice/maple/benchmark directory. The corresponding SXF lattice files are produced in /home/oxygen/XML2ADXF and /home/oxygen/ADXF2SXF/. The filenames are column headings in the following table, which contains lattice parameters, as calculated by MAPLE.
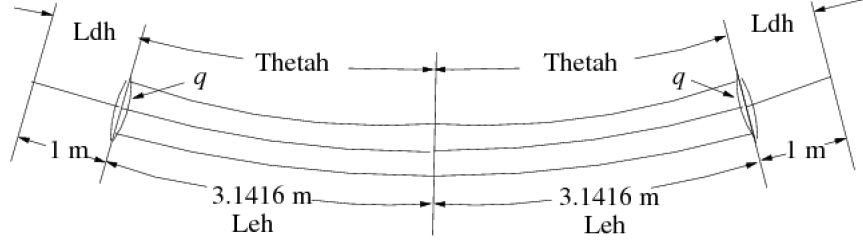
Figure 1: Single cell geometry. The full lattice consists of 40 identical cells.

Table 1: Parameters of benchmark all-electric EDM lattices, and Twiss parameters calculated from linearized transfer matrices. Note that the "half bend", and "half drift" elements are treated as individual elements in the sxf file. This gives 80 bends. The software treats these as 160 bends after slicing.

file name	variable name	unit	E_BM_M1.0.sxf	E_BM_Z.sxf	E_BM_P1.0.sxf
cells/arc	NCellPerArc		20	20	20
bend radius	r0	m	40.0	40.0	40.0
half drift length	Ldh	m	1.0	1.0	1.0
half bend per cell	Thetah	r	0.078539816	0.078539816	0.078539816
half bend length	Leh	m	3.141592	3.141592	3.141592
circumference	circum	m	331.327	331.327	331.327
inverse focal length	q	1/m	-0.002019	-0.00005960	0.0019075
field index	m		-1.0	1.0e-10	1.0
horizontal beta	betax	m	35.9237	36.1018	36.1910
vertical beta	betay	m	264.182	263.620	262.237
horizontal tune	Qx		1.4605	1.4578	1.4588
vertical tune	Qy		0.20024	0.20004	0.20047

3   Twiss Parameter Extraction

A once-around ("monodromy" in mathematical terminology) transfer matrix at any point in the ring has the standard Twiss parameterization,

$$\mathbf{M} = \begin{pmatrix} \cos\mu + \alpha\sin\mu & \beta\sin\mu \\ -\frac{1+\alpha^2}{\beta}\sin\mu & \cos\mu - \alpha\sin\mu \end{pmatrix}. \tag{3}$$

At a mirror symmetry point in the lattice, as here, though not in general, α vanishes. The phase advance $\mu = 2\pi Q$ can be obtained from

$$\cos\mu = \frac{M_{11} + M_{22}}{2}, \quad \text{and} \quad M_{12} = \beta\sin\mu. \tag{4}$$

This has assumed that β is, by definition, positive. These equations determine the signs of both $\cos\mu$ and $\sin\mu$. Reading counter-clockwise, the four consecutive phase space quadrants, I/II/III/IV, are characterized by cosine, sine sign pairs ++/-+/- -/+-, respectively.

3

We then obtain the fractional parts of the phase advance from

$$
\mu = \begin{cases} \cos^{-1}(\frac{M_{11}+M_{22}}{2}), & \text{if quadrant is I or II} \\ 2\pi - \cos^{-1}(\frac{M_{11}+M_{22}}{2}), & \text{if quadrant is III or IV} \end{cases} .
\tag{5}
$$

This still only partially resolves the aliasing ambiguity. Resolving the integer tune ambiguity requires keeping track of phase space quadrants while tracking through the lattice. To avoid error in this process it is important for sampling intervals small enough that no phase quadrant can be skipped. This keeping track of the integer tune is indicated in captions to graphs below. We then obtain β from Eq. (4), and α from

$$
\alpha = \frac{M_{11} - M_{22}}{2 \sin \mu}.
\tag{6}
$$

It is because the TEAPOT family of codes use only particle tracking, and no transfer matrices in studying ring behavior—transfer matrix components, and Twiss and other lattice functions are only obtained for the purpose of comparing results with more conventional accelerator simulation codes.

4   ETEAPOT tune determinations and analytic comparisons

4.1   Data collection organization

In all cases, $m = 1, 0, -1$, the lumped Q-quadrupoles strengths, q, were adjusted to produce vertical tune $Q_y = 0.2$. Values of q are given in the graph titles. For each of the three benchmark lattices, bunches of 21 standard particles are tracked for one turn. Each of the 80 bend elements is sliced in half for this (and all other) analyses. The graphs show horizontal and vertical displacements for two of the standard particles at the exits from each of the bends. Both transverse tune determinations are shown in the figure captions.

Once-around transfer matrices are obtained from the 21 standard particles using numerical differences. This differencing is based on the smallness (typically $1\,\mu$m spatial displacement, $1\,\mu$r angular displacement) of the initial offsets. Sensitivity to this choice is investigated in Table 2 and other tables. Twiss parameters, β_x, β_y, and μ_x, μ_y are calculated using the procedures already described. The fractional and integer tunes are obtained from the graphs the following the tables.

Dependence of the lattice parameters on "differencing" displacement `tiny` are shown in Tables 2, 3, and 4.

Each bend element in any SXF lattice description file corresponds to a single bend element in an actual ring and is therefore referred to as a "single bend". By the internal construction of ETEAPOT, each such bend is sliced at least once, or (optionally) more times.

Because the "cylindrical" $m = 0$ electrode shape choice is considered to be the most favorable, more dependencies are investigated for $m = 0$ than for $m = \pm 1$. In particular the effect of "artificial pre-slicing" is investigated for $m = 0$.

4.2 Lattice E_BM_P1.0, $m = 1$, "spherical" bending results

4.2.1 Two ETEAPOT slices per bend

Table 2 shows the lattice parameters obtained with $m = 1$, "spherical" bending, with minimal ETEAPOT slicing of 2 slices per bend. ETEAPOT results agree well with analytic lattice calculations using MAPLE. The accuracy of "differentiation by differencing" is investigated. The effect of increasing the unit differencing value `tiny` $= 10^{-6}$ by two orders of manitude has negligible effect on the lattice parameters, showing that the differencing provides sufficient accuracy.

Table 2: E_TEAPOT comparisons for `./tracker ./data/E_BM_P1.0.sxf 30 1 > & !` JTout. All `typ` numerical differentiation displacements are proportional to `tiny`.

| file name	variable name	unit	linearized MAPLE	2 slices/bend ETEAPOT	Δ's
cells/arc	NCellPerArc		20		
bend radius	r0	m	40.0		
half drift length	Ldh	m	1.0		
half bend per cell	Thetah	r	0.078539816		
half bend length	Leh	m	3.141592		
circumference	circum	m	331.327		
inverse focal length	q	1/m	0.0019075		
field index	m		1.0		
tiny=1.0e-6					
horizontal beta	betax	m	36.1910	36.1910	0.0000
vertical beta	betay	m	262.2370	262.2370	0.0000
horizontal tune	Qx		1.4588	1.4588	0.0000
vertical tune	Qy		0.2005	0.2005	0.0000
tiny=1.0e-5					
horizontal beta	betax	m	36.1910	36.1910	0.0000
vertical beta	betay	m	262.2370	262.2370	0.0000
horizontal tune	Qx		1.4588	1.4588	0.0000
vertical tune	Qy		0.2005	0.2005	0.0000
tiny=1.0e-4					
horizontal beta	betax	m	36.1910	36.1925	0.0015
vertical beta	betay	m	262.2370	262.2336	-0.0034
horizontal tune	Qx		1.4588	1.4588	0.0000
vertical tune	Qy		0.2005	0.2005	0.0000
tiny=1.0e-3					
horizontal beta	betax	m	36.1910	36.3349	0.1439
vertical beta	betay	m	262.2370	261.8966	-0.3404
horizontal tune	Qx		1.4588	1.4589	0.0001
vertical tune	Qy		0.2005	0.2006	0.0001
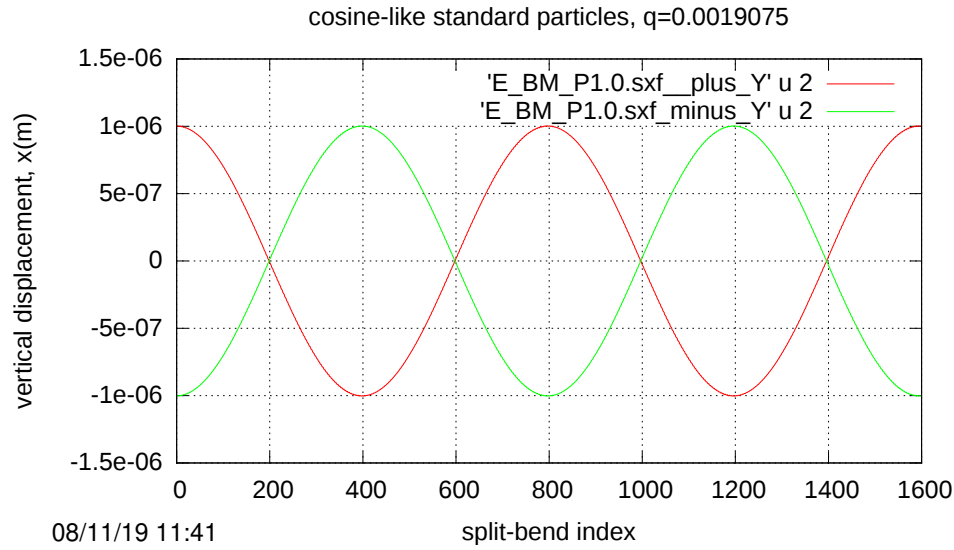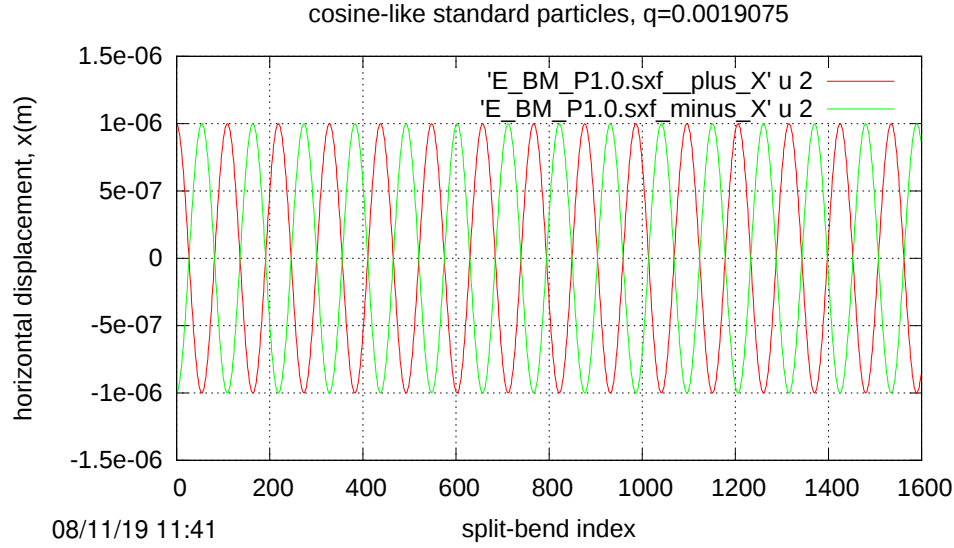
Figure 2: Lattice E_BM_P1.0.sxf; Upper: Horizontal Displacement: 10 turns, 1 sample per split bend. $Q_x \approx 14.5$ osc/10turns=1.45 osc/turn. The integer part of the tune is $[Q_x] = 1$. Lower: Vertical Displacement: 10 turns, 1 sample per split bend. $Q_y \approx 2.0$ osc/10turns=0.20 osc/turn. The integer part of the tune is $[Q_y] = 0$.

6

4.3 Lattice E_BM_Z, $m = 0$, "cylindrical" bending results

4.3.1 Two TEAPOT slices per bend

Table 3 shows the lattice parameters obtained with $m = 0$, "cylindrical" bending, with minimal ETEAPOT slicing of 2 slices per bend. Differences between MAPLE theory and ETEAPOT are shown in the final column of Table 3, though quite small, are not nearly as small as those obtained in Table 2. What makes this "not-very-surprising" is the fact that ETEAPOT evaluates all lattice parameters as "perturbations" caused by m-value deviation away from $m = 1$—this deviation vanishes for the results in Table 3. By comparing values in these two tables the relative importance of differencing and first order perturbation can be estimated.

Table 3: E_TEAPOTComparisons for ./tracker ./data/E_BM_Z.sxf 30 0 > & ! JTout. All typ numerical differentiation displacements are proportional to tiny.

file name	variable name	unit	linearized MAPLE	2 slices/bend ETEAPOT	Δ's
cells/arc	NCellPerArc		20		
bend radius	r0	m	40.0		
half drift length	Ldh	m	1.0		
half bend per cell	Thetah	r	0.078539816		
half bend length	Leh	m	3.141592		
circumference	circum	m	331.327		
inverse focal length	q	1/m	-0.00005960		
field index	m		1.0e-10		
tiny=1.0e-6					
horizontal beta	betax	m	36.1018	36.0795	-0.0223
vertical beta	betay	m	263.6200	261.4688	-2.1512
horizontal tune	Qx		1.4578	1.4581	0.0003
vertical tune	Qy		0.2000	0.2018	0.0018
tiny=1.0e-5					
horizontal beta	betax	m	36.1018	36.0795	-0.0223
vertical beta	betay	m	263.6200	261.4688	-2.1512
horizontal tune	Qx		1.4578	1.4581	0.0003
vertical tune	Qy		0.2000	0.2018	0.0018
tiny=1.0e-4					
horizontal beta	betax	m	36.1018	36.0809	-0.0209
vertical beta	betay	m	263.6200	261.4654	-2.1546
horizontal tune	Qx		1.4578	1.4581	0.0003
vertical tune	Qy		0.2000	0.2018	0.0018
tiny=1.0e-3					
horizontal beta	betax	m	36.1018	36.2190	0.1172
vertical beta	betay	m	263.6200	261.1318	-2.4882
horizontal tune	Qx		1.4578	1.4582	0.0004
vertical tune	Qy		0.2000	0.2019	0.0019

cosine-like standard particles, q=-0.0000596

cosine-like standard particles, q=-0.0000596
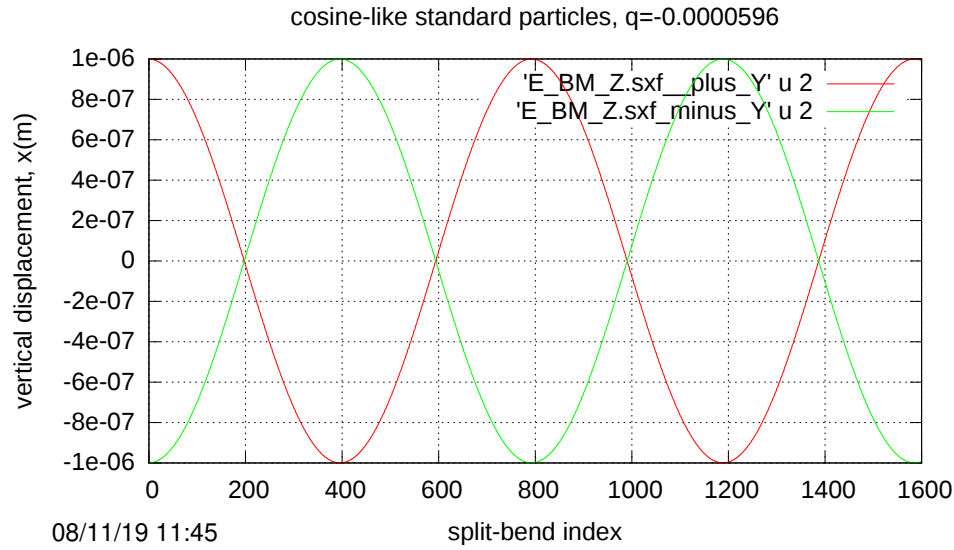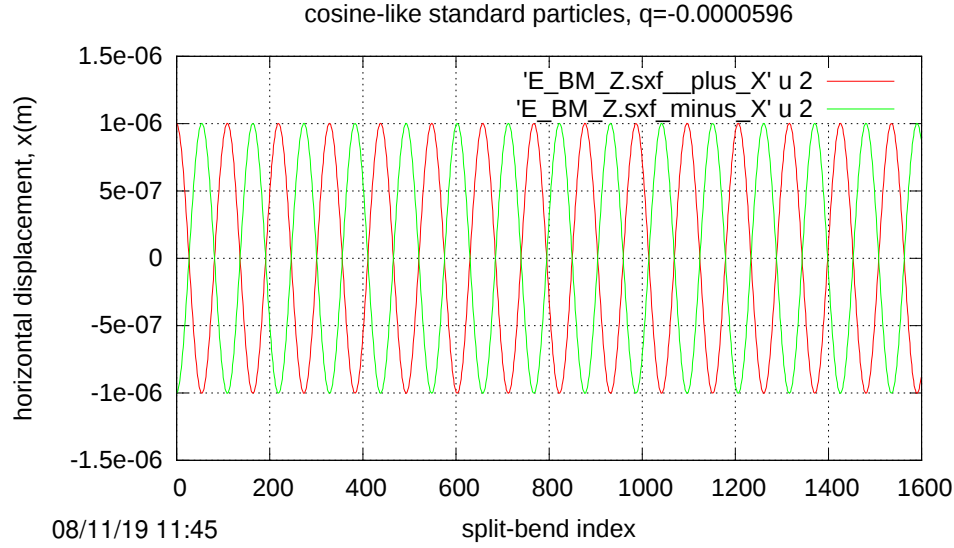
Figure 3: Lattice E_BM_Z.sxf: Upper: Horizontal Displacement: 10 turns, 1 sample per bend. $Q_x \approx 14.5$ osc/10turns=1.45 osc/turn. The integer part of the tune is $[Q_x] = 1$. Lower: Vertical Displacement: 10 turns, 1 sample per bend. $Q_y \approx 2.0$ osc/10turns=0.20 osc/turn. The integer part of the tune is $[Q_y] = 0$.

4.3.2 Ten SXF slices per bend, each with two TEAPOT slices

This section investigates the properties of a "pre-sliced" SXF lattice `E-BM-Z-sl.sxf`, which is the same as lattice `E-BM-Z.sxf` except for having all bends pre-sliced into ten slices. Though there is little horizontal effect, Figure 4 shows that the pre-slicing has actually caused the lattice to be vertically unstable. This reflects the extremely weak vertical focusing.
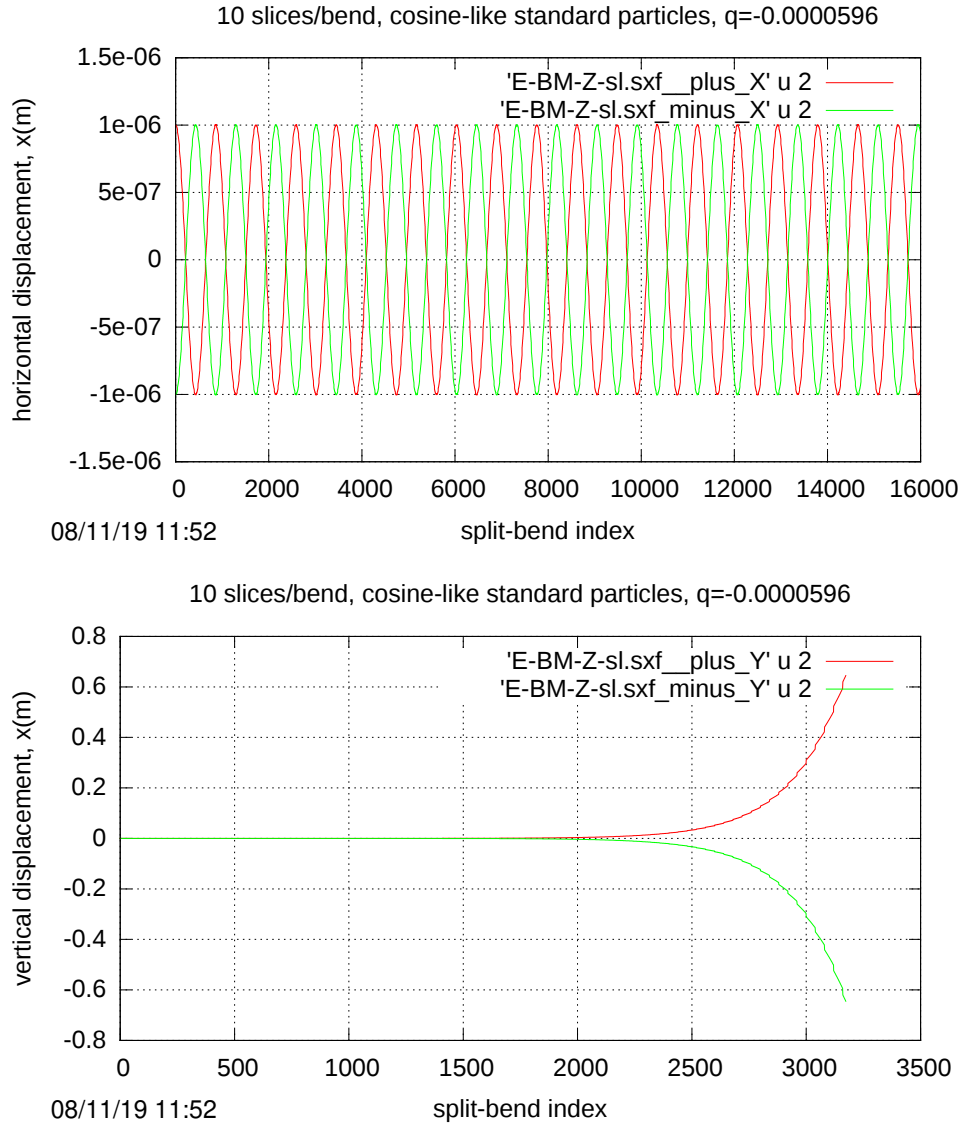

Figure 4: E_BM_Z-sl.sxf:

4.3.3 Ten SXF slices per bend, each with two TEAPOT slices, retuned q-value

To restore vertical stability the lumped quadrupole value has been adjusted from $q = -0.0000596$ to $q = -0.002020$, which correspods to focal length $f = 1/q \approx 500\,\text{m}$, and is quite weak for a six meter long cell length.
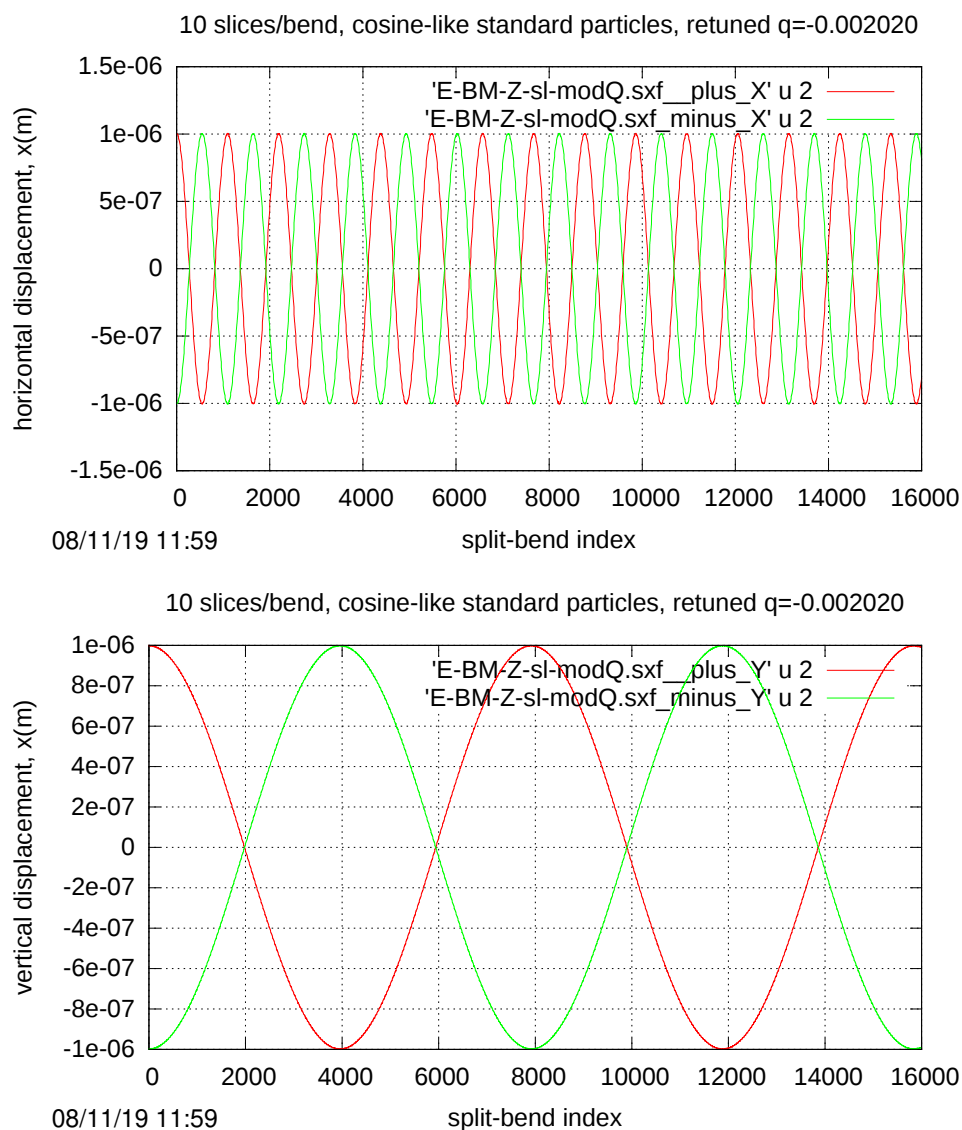

Figure 5: `E_BM_Z-sl-modQ.sxf`:

4.4 Lattice E_BM_M1.0, $m = -1$, bending results

Table 4: E_TEAPOT comparisons for `./tracker ./data/E_BM_M1.0.sxf 30 -1 > & !
JTout`. All `typ` numerical differentiation displacements are proportional to `tiny`.

file name	variable name	unit	linearized MAPLE	2 slices/bend ETEAPOT	Δ's
cells/arc	NCellPerArc		20		
bend radius	r0	m	40.0		
half drift length	Ldh	m	1.0		
half bend per cell	Thetah	r	0.078539816		
half bend length	Leh	m	3.141592		
circumference	circum	m	331.327		
inverse focal length	q	1/m	-0.002019		
field index	m		-1.0		
tiny=1.0e-6					
horizontal beta	betax	m	35.9237	35.8566	-0.0671
vertical beta	betay	m	264.1820	251.8522	-12.3298
horizontal tune	Qx		1.4605	1.4620	0.0015
vertical tune	Qy		0.2002	0.2102	0.0100
tiny=1.0e-5					
horizontal beta	betax	m	35.9237	35.8566	-0.0671
vertical beta	betay	m	264.1820	251.8522	-12.3298
horizontal tune	Qx		1.4605	1.4620	0.0015
vertical tune	Qy		0.2002	0.2102	0.0100
tiny=1.0e-4					
horizontal beta	betax	m	35.9237	35.8582	-0.0655
vertical beta	betay	m	264.1820	251.8492	-12.3328
horizontal tune	Qx		1.4605	1.4620	0.0015
vertical tune	Qy		0.2002	0.2102	0.0100
tiny=1.0e-3					
horizontal beta	betax	m	35.9237	36.0209	0.0972
vertical beta	betay	m	264.1820	251.5553	-12.6267
horizontal tune	Qx		1.4605	1.4621	0.0016
vertical tune	Qy		0.2002	0.2103	0.0101

cosine-like standard particles, q=-0.002019

cosine-like standard particles, q=-0.002019
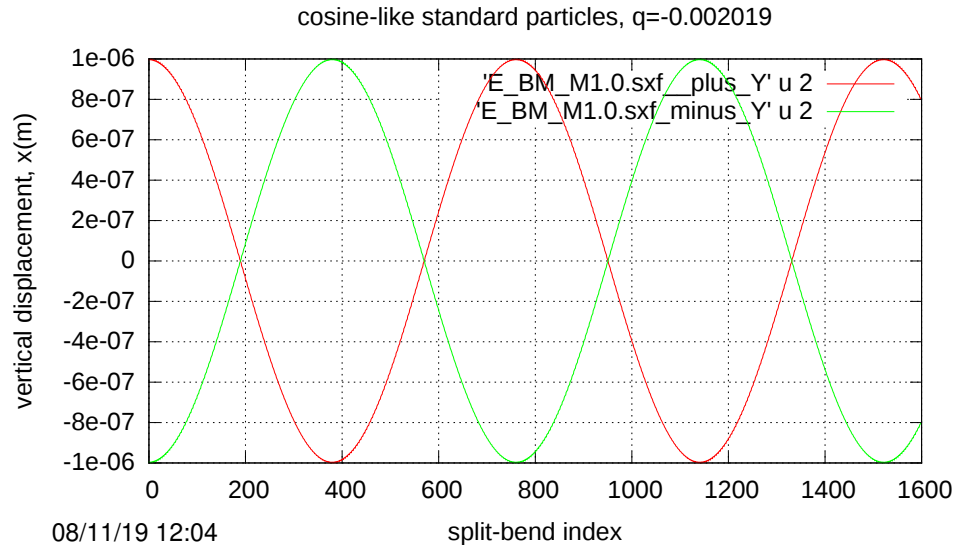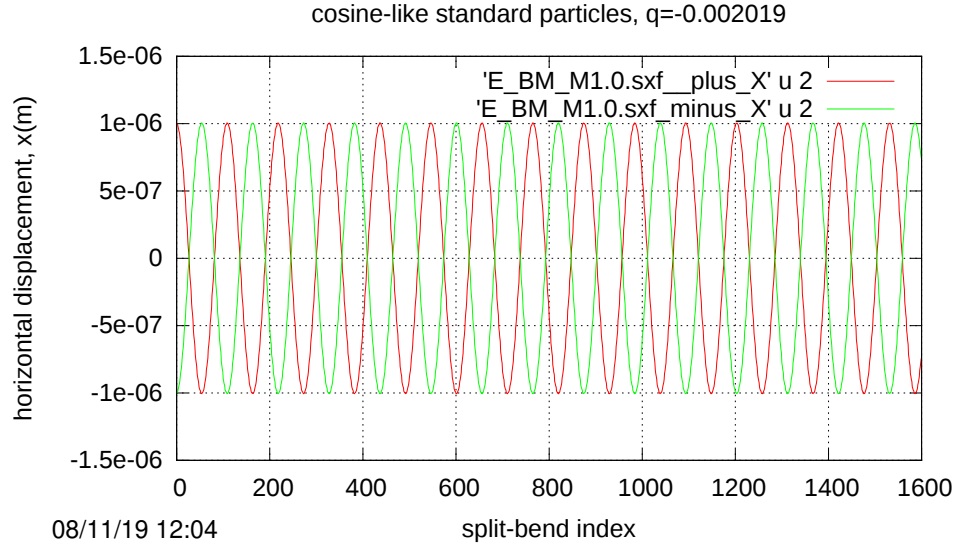
Figure 6: E_BM_M1.0.sxf: Horizontal Displacement: 10 turns, 1 sample per bend. $Q_x \approx$ 14.5 osc/10turns=1.45 osc/turn. The integer part of the tune is $[Q_x] = 1$. Vertical Displacement: 10 turns, 1 sample per bend. $Q_y \approx 2.1$ osc/10turns=0.21 osc/turn. The integer part of the tune is $[Q_y] = 0$.

12

4.5 Dependence on ETEAPOT Slicing Granularity

The effect of finer ETEAPOT slicing is investigated in Tables 5, 6 and 7. Doubling the slicing from 2 slices/bend to 4 slices/bend has little effect on the derived lattice parameters. As in earlier parameter determinations, the vanishing differences for $m = 1$ suggest that the main deviations are due more to perturbation away from $m = 1$ than to overly-coarse slicing.

Table 5: E_TEAPOT comparisons for `./tracker ./data/E_BM_P1.0.sxf 30 1 > & !` JTout. tiny=1.0e-6.

file name	variable name	unit	linearized	2 sl./bend	Δ's	4 sl./bend	Δ's
cells/arc	NCellPerArc		20				
bend radius	r0	m	40.0				
half drift length	Ldh	m	1.0				
half bend per cell	Thetah	r	0.078539816				
half bend length	Leh	m	3.141592				
circumference	circum	m	331.327				
inverse focal length	q	1/m	0.0019075				
field index	m		1.0				
horizontal beta	betax	m	36.191030	36.19103		36.19103	
vertical beta	betay	m	262.236988	262.23701		262.23701	
horizontal tune	Qx		1.458782	1.45878		1.45878	
vertical tune	Qy		0.200472	0.20047		0.20047	

Table 6: E_TEAPOT comparisons for `./tracker ./data/E_BM_Z.sxf 30 0 > & !` JTout. tiny=1.0e-6.

file name	variable name	unit	linearized	2 sl./bend	Δ's	4 sl./bend	Δ's
cells/arc	NCellPerArc		20				
bend radius	r0	m	40.0				
half drift length	Ldh	m	1.0				
half bend per cell	Thetah	r	0.078539816				
half bend length	Leh	m	3.141592				
circumference	circum	m	331.327				
inverse focal length	q	1/m	-0.00005960				
field index	m		1.0e-10				
horizontal beta	betax	m	36.101819	36.07949		36.09624	
vertical beta	betay	m	263.620065	261.46880		263.07673	
horizontal tune	Qx		1.457801	1.45813		1.45788	
vertical tune	Qy		0.200044	0.20177		0.20048	

Table 7: E_TEAPOT comparisons for `./tracker ./data/E_BM_M1.0.sxf 30 -1 > & !` JTout. `tiny=1.0e-6`.

file name	variable name	unit	linearized	2 sl./bend	Δ's	4 sl./bend	Δ's
cells/arc	NCellPerArc		20				
bend radius	r0	m	40.0				
half drift length	Ldh	m	1.0				
half bend per cell	Thetah	r	0.078539816				
half bend length	Leh	m	3.141592				
circumference	circum	m	331.327				
inverse focal length	q	1/m	-0.002019				
field index	m		-1.0				
horizontal beta	betax	m	35.923719	35.85659		35.90695	
vertical beta	betay	m	264.182337	251.85222		260.92409	
horizontal tune	Qx		1.460454	1.46204		1.46085	
vertical tune	Qy		0.200242	0.21021		0.20278	

5 Comments and Conclusions

For the $m = 1$ case, there is nearly exact agreement between the linearized analytic formulae and the tracking formalism. This is "as should be", but far from automatic. The equations of the linearized transfer matrix formalism and the arbitrary-amplitude Munoz-Pavic seem utterly different. So the close agreement confirms *both* approaches. This comment mainly applies to the "in-plane" horizontal motion. Agreement of the "out-of-plane" vertical motion, where the overall agreement is less impressive, especially as investigated with a pre-sliced SXF lattice, in Sections 4.3.2 and 4.3.3. Vertical steering errors, however small, are amplified by the weak vertical focusing of the lattice.

The agreement for $m \neq 1$ is excellent, but clearly not as good as for $m = 1$. This strongly suggests that the (artificial) perturbative kick compensation is not quite perfect. It is also not surprising that the deviation is proportional to $(m - 1)^2$; and that, for $m = 1$, the kick correction strength vanishes.

For most practical purposes, the code performance in the parameter range $-1 \leq m \leq 1$ has been shown to be satisfactory.

References

[1] Storage Ring EDM Collaboration, *A Proposal to Measure the Proton Electric Dipole Moment with 10^{-29} e-cm Sensitivity*, especially Appendix 1. October, 2011

[2] C. Møller, *The Theory of Relativity*, Clarendon Press, Oxford, 1952,

[3] G. Muñoz and I. Pavic, *A Hamilton-like vector for the special-relativistic Coulomb problem*, Eur. J. Phys. **27**, 1007-1018, 2006

[4] R. Talman, *Geometric Mechanics,* John Wiley and Sons, 2000

[5] J. Aguirregabiria et al., Archiv:physics/0407049v1 [physics.ed-ph] 2004,

[6] U. Torkelsson, Eur. J. Phys., **19**, 459, 1998,

[7] T. Boyer, Am. J. Phys. **72** (8) 992, 2004